oxidation. Translation of taxonomic information into phenotype profiles based on experimental evidence can thus facilitate the ecological interpretation of metagenomes. The full potential of phenotype profiling remains underused because of our current inability to associate many known taxa with any function. For example, a large fraction of the ubiquitous but poorly studied phylum Thaumarchaeota is potentially involved in ammonia oxidation (*24*) but had to be excluded from our functional annotations (*11*). Similarly, microeukaryotes likely contribute to several metabolic functions, such as photosynthesis or cellulolysis. Future functional profiling should thus include eukaryotic microorganisms and incorporate putative metabolic potential for uncultured clades revealed by single-cell genomics (*25*).

The bulk of global biogeochemical fluxes is driven by a core set of metabolic pathways that evolved in response to past geochemical conditions (*1*). Through time, these pathways have spread across microbial clades that compete within metabolic niches, resulting in an enormous microbial diversity characterized by high functional redundancy. As shown here, splitting variation of microbial community composition into variation of functional structure and taxonomic variation within functional groups reveals an intriguing pattern: The functional component in itself captures most of the variation predicted by environmental conditions, whereas the residual component (i.e., variation within functional groups) only weakly relates to environmental conditions. This has implications for the interpretation of differences in community structure across environments and time. Differences in taxonomic composition that do not affect functional composition may have little relevance to ecosystem biochemistry; conversely, physicochemically similar environments could host taxonomically distinct communities (*26*). Functional (rather than purely taxonomic) descriptions of microbial communities should therefore constitute the baseline for microbial biogeography, particularly across transects where geochemical gradients shape microbial niche distribution (*27*). The residual variation within functional groups can then be analyzed separately to elucidate additional community assembly mechanisms such as biotic interactions, dispersal limitation, or demographic drift. An incorporation of global microbial functional profiles, and their response to potentially changing environmental conditions, into future biogeochemical models will greatly benefit reconstructive and predictive modeling of Earth's elemental cycles.

REFERENCES AND NOTES

1. P. G. Falkowski, T. Fenchel, E. F. Delong, *Science* **320**, 1034–1039 (2008).
2. E. F. DeLong *et al.*, *Science* **311**, 496–503 (2006).
3. J. A. Fuhrman, *Nature* **459**, 193–199 (2009).
4. J. B. H. Martiny *et al.*, *Nat. Rev. Microbiol.* **4**, 102–112 (2006).
5. S. L. Strom, *Science* **320**, 1043–1045 (2008).
6. P. Larsen, Y. Hamada, J. Gilbert, *J. Biotechnol.* **160**, 17–24 (2012).
7. G. Lima-Mendez *et al.*, *Science* **348**, 1262073 (2015).
8. I. D. Ofiteru *et al.*, *Proc. Natl. Acad. Sci. U.S.A.* **107**, 15345–15350 (2010).
9. J. B. H. Martiny, S. E. Jones, J. T. Lennon, A. C. Martiny, *Science* **350**, aac9323 (2015).
10. J. Raes, I. Letunic, T. Yamada, L. J. Jensen, P. Bork, *Mol. Syst. Biol.* **7**, 473 (2011).
11. See supplementary materials on *Science* Online.
12. F. O. Aylward *et al.*, *Proc. Natl. Acad. Sci. U.S.A.* **112**, 5443–5448 (2015).
13. P. E. Larsen, D. Field, J. A. Gilbert, *Nat. Methods* **9**, 621–625 (2012).
14. S. Sunagawa *et al.*, *Science* **348**, 1261359 (2015).
15. S. M. Gibbons *et al.*, *Proc. Natl. Acad. Sci. U.S.A.* **110**, 4651–4655 (2013).
16. C. A. Suttle, *Nat. Rev. Microbiol.* **5**, 801–812 (2007).
17. C. Burke, P. Steinberg, D. Rusch, S. Kjelleberg, T. Thomas, *Proc. Natl. Acad. Sci. U.S.A.* **108**, 14288–14293 (2011).
18. A. Ramette, *FEMS Microbiol. Ecol.* **62**, 142–160 (2007).
19. D. Aguilar, F. X. Aviles, E. Querol, M. J. E. Sternberg, *J. Mol. Biol.* **340**, 491–512 (2004).
20. J. J. Morris, R. E. Lenski, E. R. Zinser, *MBio* **3**, e00036-12 (2012).
21. J. I. Prosser, *Nat. Rev. Microbiol.* **13**, 439–446 (2015).
22. A. L. Müller, K. U. Kjeldsen, T. Rattei, M. Pester, A. Loy, *ISME J.* **9**, 1152–1165 (2015).
23. M. G. Langille *et al.*, *Nat. Biotechnol.* **31**, 814–821 (2013).
24. D. A. Stahl, J. R. de la Torre, *Annu. Rev. Microbiol.* **66**, 83–101 (2012).
25. P. C. Blainey, *FEMS Microbiol. Rev.* **37**, 407–427 (2013).
26. A. Fernández *et al.*, *Appl. Environ. Microbiol.* **65**, 3697–3704 (1999).
27. J. L. Green, B. J. Bohannan, R. J. Whitaker, *Science* **320**, 1039–1043 (2008).
28. E. Pruesse *et al.*, *Nucleic Acids Res.* **35**, 7188–7196 (2007).

ACKNOWLEDGMENTS

We thank S. P. Otto, A. L. González, M. M. Osmond, and S. J. Hallam for comments and advice. Supported by the University of British Columbia Department of Mathematics (S.L.) and the Natural Sciences and Engineering Research Council of Canada (S.L., L.W.P., and M.D.). The authors declare that they have no competing financial interests. Metagenomic sequence data are accessioned at the International Nucleotide Sequence Database Collaboration (accession numbers listed in table S2). The FAPROTAX database (Functional Annotation of Prokaryotic Taxa) and associated software, which we developed for generating the functional profiles, are freely available at www.zoology.ubc.ca/louca/FAPROTAX.

SUPPLEMENTARY MATERIALS

www.sciencemag.org/content/353/6305/1272/suppl/DC1
Materials and Methods
Tables S1 to S4
Figs. S1 to S28
References (*29*–*62*)
Additional data table S1

10 February 2016; accepted 23 August 2016
10.1126/science.aaf4507

SENSORY BIOLOGY

Bats perceptually weight prey cues across sensory systems when hunting in noise

D. G. E. Gomes,[1,2] R. A. Page,[1] I. Geipel,[1] R. C. Taylor,[1,3] M. J. Ryan,[1,4] W. Halfwerk[1,5]*

Anthropogenic noise can interfere with environmental information processing and thereby reduce survival and reproduction. Receivers of signals and cues in particular depend on perceptual strategies to adjust to noisy conditions. We found that predators that hunt using prey sounds can reduce the negative impact of noise by making use of prey cues conveyed through additional sensory systems. In the presence of masking noise, but not in its absence, frog-eating bats preferred and were faster in attacking a robotic frog emitting multiple sensory cues. The behavioral changes induced by masking noise were accompanied by an increase in active localization through echolocation. Our findings help to reveal how animals can adapt to anthropogenic noise and have implications for the role of sensory ecology in driving species interactions.

Anthropogenic noise is a globally rising environmental pollutant that has been linked to lower survival and reduced reproductive success of many animal taxa (*1*–*3*). Noise can mask environmental cues, making it difficult to hear moving prey or approaching predators, and can interfere with the perception of acoustic communication signals (*3*–*6*). Signal producers may be able to reduce the masking impact—for example, by calling louder (*7*–*9*)—but such signaling strategy is unavailable to receivers. Some receivers can depend on perceptual strategies to maintain cue detection and thereby adapt to noisy environments (*10*, *11*).

Predators such as bats and owls are highly specialized to hunt prey by ear (*12*); thus, noise that masks prey sounds severely hampers their foraging success (*4*, *5*). However, predators may be able to adapt to masking levels of anthropogenic noise by actively shifting their attention or emphasis placed on processing cues from different sensory modalities from the same prey (*13*–*16*). We refer to this as cross-modal perceptual weighting (*17*).

We studied the effect of masking noise on the attack behavior of the fringe-lipped bat (*Trachops cirrhosus*), a neotropical species that is specialized

[1]Smithsonian Tropical Research Institute, Apartado 0843-03092 Balboa, Panama. [2]Max Planck Institute for Ornithology, Seewiesen 82319, Germany. [3]Department of Biology, Salisbury University, Salisbury, MD 21801, USA. [4]Department of Integrative Biology, University of Texas, Austin, TX 78712, USA. [5]Department of Ecological Science, VU University, Amsterdam 1081 HV, Netherlands.
***Corresponding author. Email: w.h.halfwerk@vu.nl**

to find frogs by eavesdropping on their mating displays (*18*, *19*). Bats can passively locate their prey using only prey-generated sounds, but their performance is severely hampered when exposed to noise (*20*). A male frog, however, provides additional, multimodal cues to hunting bats, as it inflates and deflates a vocal sac while calling (*14*, *16*). Bats can detect the frog's vocal sac with their echolocation (i.e., processing the ultrasonic echoes that return from their prey), but only when the sac is dynamically inflated; bats do not detect a static vocal sac (*21*). Echolocation

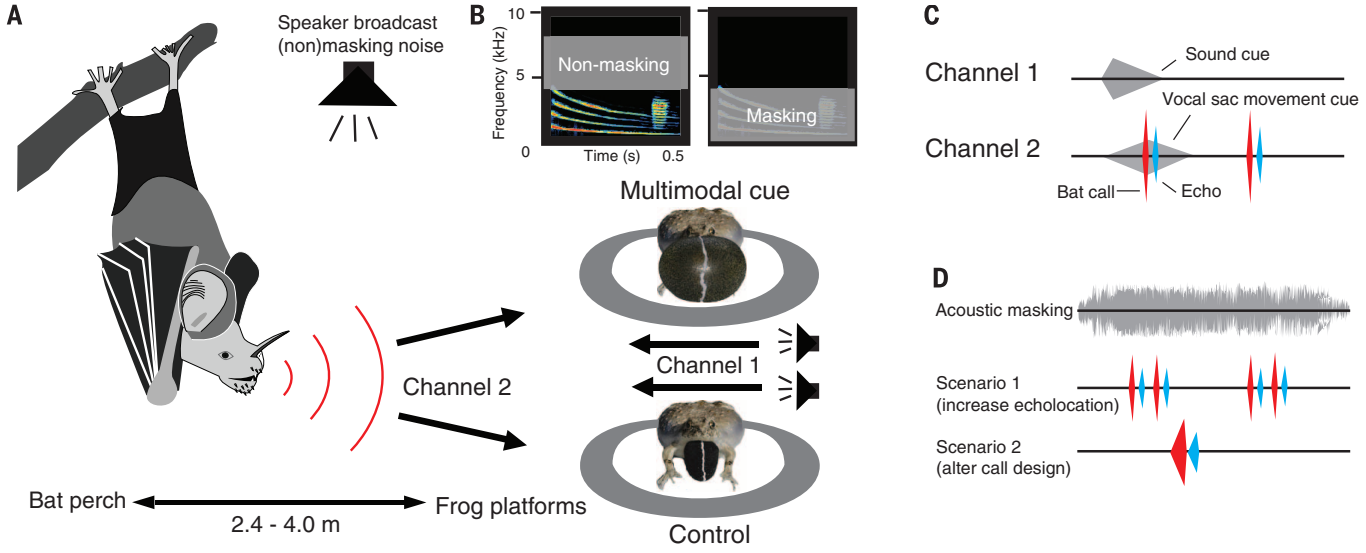

Fig. 1. Perceptual strategies to deal with prey signal masking. (**A**) Graphic representation of our experimental design. Bats can passively listen to frog sounds (channel 1) broadcast from speakers underneath the robofrog models; they can also actively use their echolocation (channel 2) to detect the dynamic vocal sac. (**B**) Bats were tested under nonmasking noise, masking noise, and control conditions (no noise) broadcast from a speaker placed above the frog models. Shown are two spectrograms of a frog call with frequency regions of noise treatments superimposed on it (4.0 to 8.0 kHz. 0.1 to 4.0 kHz). (**C**) Bats can rely on passive listening to their prey's mating sound (channel 1) as well as on active listening by processing multiple echoes returning from the frog's moving vocal sac (channel 2). Shown are the typical frog call amplitude profile (channel 1), the inflation and deflation of the frog's vocal sac (channel 2, gray symbol), and bat calls (red symbols) and echoes (blue symbols) overlapping as well as nonoverlapping in time with the vocal sac cue. (**D**) When noise masks the prey call, bats may increase their echolocation effort (scenario 1) or alter call design (scenario 2) to maintain target localization.

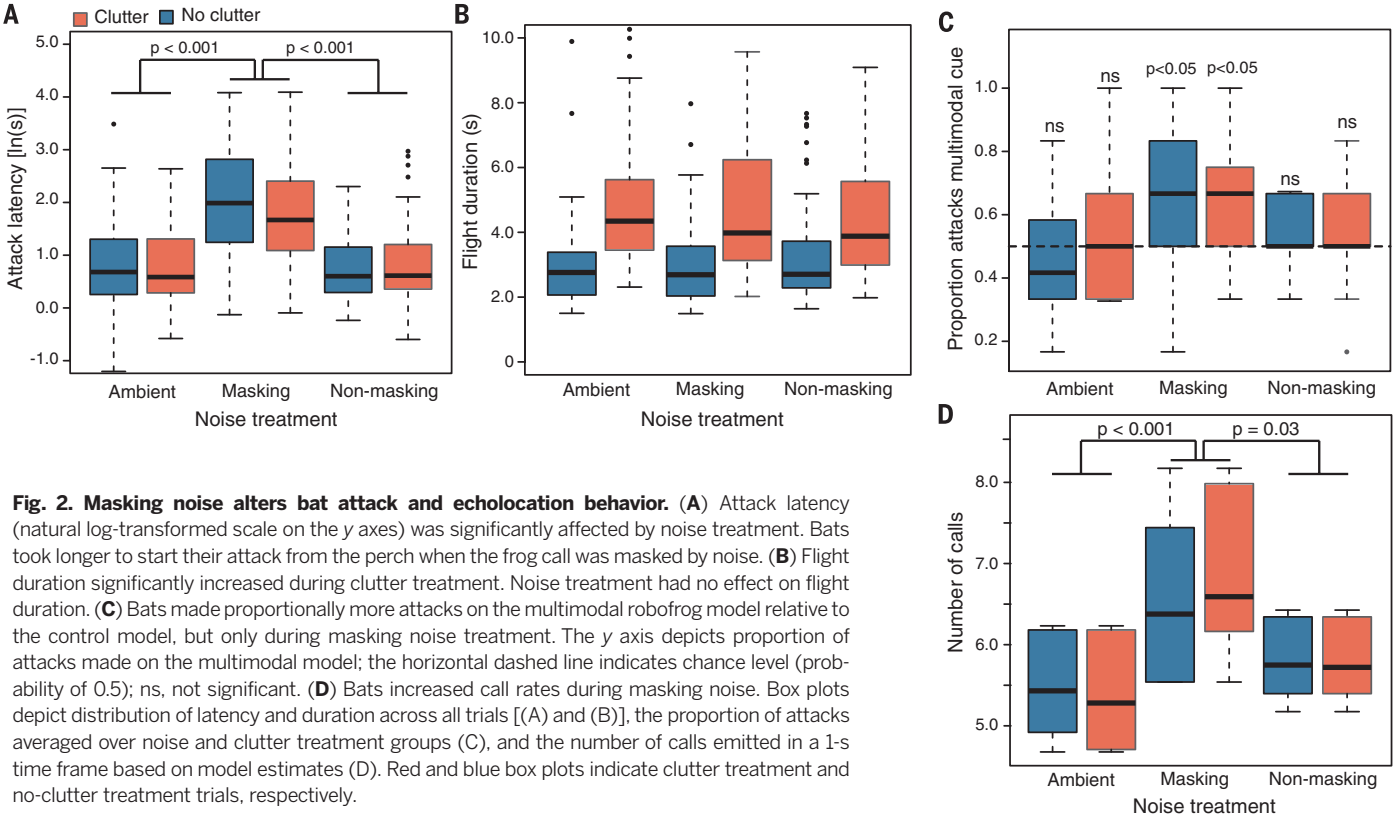

Fig. 2. Masking noise alters bat attack and echolocation behavior. (**A**) Attack latency (natural log-transformed scale on the *y* axes) was significantly affected by noise treatment. Bats took longer to start their attack from the perch when the frog call was masked by noise. (**B**) Flight duration significantly increased during clutter treatment. Noise treatment had no effect on flight duration. (**C**) Bats made proportionally more attacks on the multimodal robofrog model relative to the control model, but only during masking noise treatment. The *y* axis depicts proportion of attacks made on the multimodal model; the horizontal dashed line indicates chance level (probability of 0.5); ns, not significant. (**D**) Bats increased call rates during masking noise. Box plots depict distribution of latency and duration across all trials [(A) and (B)], the proportion of attacks averaged over noise and clutter treatment groups (C), and the number of calls emitted in a 1-s time frame based on model estimates (D). Red and blue box plots indicate clutter treatment and no-clutter treatment trials, respectively.

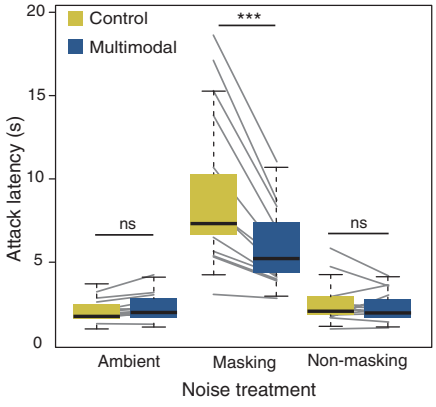

Fig. 3. Multimodal cues reduce attack latency under masking noise levels. Attack latency showed a significant interaction between noise treatment and multimodal cue use. Bats were faster in attacking the multimodal model relative to the control model only during masking noise. Box plots depict model estimates per noise treatment group and attack choice (on either the control or the multimodal model). Gray lines depict fitted slopes per individual per noise treatment. ***$P < 0.001$.

can provide highly accurate spatial information about target stimuli, and we therefore expected that these bats are capable of adapting to masking interference through a change in their perceptual weighting of sonic cues versus ultrasonic cues (*22*).

We used robotic frogs that emitted either multimodal cues (sound plus moving vocal sac) or control cues (sound plus static vocal sac) (Fig. 1A). Individual bats were given a choice to attack one of two models under three different noise treatments: (i) a masking noise overlapping the main frequency range of the frog call, (ii) a nonmasking noise, and (iii) an ambient control noise condition (Fig. 1B and supplementary materials). Although the signal-to-noise ratio of the frog call was strongly reduced during masking noise, the signal remained audible to the perched bat (Fig. 1B). We predicted that bats rely more on echolocation when presented with masking noise and would consequently make more attacks on the multimodal frog model and alter their echolocation behavior [see scenarios in Fig. 1, C and D, or (*23*)]. Objects surrounding a target also return echoes, and this so-called background clutter is known to interfere with detection and processing of echolocation target cues (*4*, *24*). We thus tested bats additionally on their attack behavior when dried leaves were added around the frog models (clutter treatment; fig. S1).

We trained 12 wild-caught bats to attack our robotic models in an outdoor flightcage (*21*). Bats always started their attack flight toward one of the frog models from their perch and only in response to stimulus playback. Attack latency was strongly influenced by our noise treatment (generalized linear mixed models, $N_{bats} = 12$, $N_{trials} = 432$, $\chi^2 = 22.07$, $P < 0.001$; Fig. 2A and table S1). Post hoc independent contrasts revealed that bats were slower in making their attacks under masking noise relative to nonmasking noise (z value = 5.57, $P < 0.001$) and ambient conditions (z value = 7.56, $P < 0.001$). We did not find a significant effect of the clutter treatment on attack latencies ($\chi^2 = 0.09$, $P = 0.76$). On the other hand, the time between leaving the perch and attack on the model (hereafter, flight duration) increased during the clutter treatment ($\chi^2 = 17.04$, $P < 0.001$; Fig. 2B) but was not affected by the noise treatment ($\chi^2 = 0.24$, $P = 0.89$). The number of attacks on the multimodal frog model relative to the control frog model was significantly affected by the noise treatment ($\chi^2 = 7.63$, $P = 0.022$; Fig. 2C). Post hoc binomial tests revealed that bats had a clear preference for the frog model displaying multimodal cues under masking noise (z value = 2.34, $P = 0.019$), but not under nonmasking noise (z value = −0.94, $P = 0.35$) or ambient conditions (z value = 1.17, $P = 0.24$). Clutter treatment had no significant effect on the probability of bat attack on either model ($\chi^2 = 0.60$, $P = 0.43$; Fig. 2C), nor did we find any significant interaction effects between noise and clutter treatment (all response variables $P > 0.5$).

We obtained ultrasonic recordings for a subset of six individuals and analyzed all calls made on the perch between stimulus onset and start of the attack flight. Bats made on average 7.69 ± 2.78 calls on their perch, the majority (77%) during the last second. We selected three calls from a 1-s portion of the recording (shortly before bats had taken flight) to test for an effect of experimental treatment on echolocation behavior. We found the number of calls produced at the perch, as well as the call rate, to be significantly affected by noise treatment (number of perch calls, $N_{bats} = 6$, $N_{trials} = 146$, $\chi^2 = 6.44$, $P = 0.039$; call rate during last second, $\chi^2 = 7.78$, $P = 0.022$; Fig. 2D). Bats increased their use of echolocation during masking noise relative to nonmasking noise (5 of 6 bats on average increased call rate; z value = 2.34, $P = 0.032$) and relative to ambient noise conditions (6 of 6 bats increased call rate; z value = 3.46, $P < 0.001$). We did not find any differences in call peak frequency ($\chi^2 = 0.27$, $P = 0.87$) or call duration ($\chi^2 = 2.85$, $P = 0.24$) between noise treatment groups. Clutter treatment had no significant effect on the number of calls emitted from the perch ($\chi^2 = 1.53$, $P = 0.22$) or on call rate ($\chi^2 = 1.26$, $P = 0.26$), call peak frequency ($\chi^2 = 1.53$, $P = 0.22$), or call duration ($\chi^2 = 0.84$, $P = 0.36$).

Masking noise increased attack latencies during our experiment, but bats could reduce this effect when using multimodal cues. We reanalyzed the attack latency data and added robofrog choice (control or multimodal) to our statistical model as an additional factor. We found a significant interaction effect between noise treatment and robofrog choice ($N_{bats} = 12$, $N_{trials} = 432$, df = 2, $\chi^2 = 11.82$, $P = 0.003$; Fig. 3 and table S1). Bats were faster in attacking the multimodal model relative to the control model, but only under masking noise levels (z value = −3.78, $P < 0.001$). Robofrog choice had no effect on attack latencies under nonmasking noise (z value = 0.86, $P = 0.78$) and ambient noise conditions (z value = −0.26, $P = 0.99$).

Anthropogenic noise can affect predator-prey dynamics through masking of acoustic cues or by distracting or disturbing individuals (*2*, *25*, *26*). Our results confirm a masking impact of noise on bat attack latencies, thereby giving frogs more time to escape predation. More important, the results show that bats can actively compensate the masking impact by making more use of cues available to them in an additional, less noisy sensory channel. We also found a factor of 2 increase in attack preferences on the multimodal versus the unimodal model, which suggests that noise can drive selection pressures acting on sexual signals.

A previous study on a bat species that echolocates silent prey showed that the negative impact of noise on hunting success is enhanced when individuals are tested in a highly cluttered environment (*4*). Clutter treatment in our experiment affected flight duration but surprisingly had no effect on attack choice or latency. Fringe-lipped bats can detect and localize the frog's vocal sac at distances up to 6 m from their perch (*21*, *22*), and it is likely that its movement allows bats to discriminate target echoes from the stationary background (*27*), such as the dried leaves we placed around our models during clutter treatment.

In conclusion, we showed that bats preferred multimodal displays to unimodal displays, but only under masking noise conditions. Such cross-modal perceptual weighting reduces the masking impact of noise and could be a general receiver strategy (*11*, *28*). A shift in the use of signals and cues across sensory systems will also alter selection pressures acting on sexual displays (*29*, *30*). Thus, in noisy human-impacted areas such as in cities or along highways, we would expect to find a change in the multimodal content of communication signals (*11*). We may also expect a shift in species composition in noisier areas based on perceptual as well as communicative traits. Species that can rapidly alter their perceptual mechanisms will likely do better in noise-impacted areas, and this in turn has consequences for their predator and prey species that emit different signals and cues. Human-induced changes to the sensory ecology of particular habitats can thus be an important factor in driving species interactions and ultimately determining community assemblages.

REFERENCES AND NOTES

1. J. P. Swaddle *et al.*, *Trends Ecol. Evol.* **30**, 550–560 (2015).
2. S. D. Simpson *et al.*, *Nat. Commun.* **7**, 10544 (2016).
3. H. E. Ware, C. J. McClure, J. D. Carlisle, J. R. Barber, *Proc. Natl. Acad. Sci. U.S.A.* **112**, 12105–12109 (2015).
4. J. Luo, B. M. Siemers, K. Koselj, *Global Change Biol.* **21**, 3278–3289 (2015).
5. B. M. Siemers, A. Schaub, *Proc. R. Soc. B* **278**, 1646–1652 (2011).
6. W. Halfwerk *et al.*, *Proc. Natl. Acad. Sci. U.S.A.* **108**, 14549–14554 (2011).
7. H. Brumm, *J. Anim. Ecol.* **73**, 434–440 (2004).
8. J. Luo, H. R. Goerlitz, H. Brumm, L. Wiegrebe, *Sci. Rep.* **5**, 18556 (2015).
9. W. Halfwerk, A. M. Lea, M. Guerra, R. A. Page, M. J. Ryan, *Behav. Ecol.* **27**, 669–676 (2016).
10. H. Brumm, H. Slabbekoorn, *Adv. Stud. Behav.* **35**, 151–209 (2005).

11. W. Halfwerk, H. Slabbekoorn, *Biol. Lett.* **11**, 20141051 (2015).
12. T. H. Kunz, M. B. Fenton, *Bat Ecology, Vol. 1* (Univ. of Chicago Press, 2006).
13. E. A. Hebets *et al.*, *Proc. R. Soc. B* **283**, 20152889 (2016).
14. R. C. Taylor, M. J. Ryan, *Science* **341**, 273–274 (2013).
15. N. E. Munoz, D. T. Blumstein, *Behav. Ecol.* **23**, 457–462 (2012).
16. W. Halfwerk, P. L. Jones, R. C. Taylor, M. J. Ryan, R. A. Page, *Science* **343**, 413–416 (2014).
17. B. E. Stein, *The New Handbook of Multisensory Processing* (MIT Press, 2012).
18. M. D. Tuttle, M. J. Ryan, *Science* **214**, 677–678 (1981).
19. J. J. Falk *et al.*, *Proc. R. Soc. B* **282**, 20150520 (2015).
20. R. A. Page, M. J. Ryan, *Anim. Behav.* **76**, 761–769 (2008).
21. W. Halfwerk *et al.*, *J. Exp. Biol.* **217**, 3038–3044 (2014).
22. F. Rhebergen, R. C. Taylor, M. J. Ryan, R. A. Page, W. Halfwerk, *Proc. R. Soc. B* **282**, 20151403 (2015).
23. K. Hulgard, J. M. Ratcliffe, *Sci. Rep.* **6**, 21500 (2016).
24. R. Arlettaz, G. Jones, P. A. Racey, *Nature* **414**, 742–745 (2001).
25. J. Purser, A. N. Radford, *PLOS ONE* **6**, e17478 (2011).
26. A. A. Chan, P. Giraldo-Perez, S. Smith, D. T. Blumstein, *Biol. Lett.* **6**, 458–461 (2010).
27. H. R. Goerlitz, C. Geberl, L. Wiegrebe, *J. Acoust. Soc. Am.* **128**, 1467–1475 (2010).
28. W. H. Sumby, I. Pollack, *J. Acoust. Soc. Am.* **26**, 212 (1954).
29. I. Starnberger, D. Preininger, W. Hödl, *J. Comp. Physiol. A* **200**, 777–787 (2014).
30. J. Heuschele, M. Mannerla, P. Gienapp, U. Candolin, *Behav. Ecol.* **20**, 1223–1227 (2009).

ACKNOWLEDGMENTS

For support in the field, we thank the Gamboa Bat Lab, specifically L. F. Gómez-Feuillet. We thank B. Klein, P. Clements, and Moey Inc. for fabricating the pneumatic robotic frog system, and J. Ellers and H. Goerlitz for comments that substantially improved the manuscript. Supported by a Smithsonian fellowship (W.H.), NSF grant IOS 1120031 (R.C.T., M.J.R., and R.A.P.), and the Smithsonian Tropical Research Institute (R.A.P.). All research reported here complied with STRI IACUC protocols (2015-0209-2018; 2014-0101-2017). We obtained all required permits from the Government of Panama (SE/A-86-14). The authors report no conflict of interest. Raw data are available at the Dryad Data Repository (dx.doi:10.5061/dryad.5gk8j).

SUPPLEMENTARY MATERIALS

www.sciencemag.org/content/353/6305/1277/suppl/DC1
Materials and Methods
Fig. S1
Table S1
References (*31*–*33*)

31 March 2016; accepted 17 August 2016
10.1126/science.aaf7934

BRAIN MICROCIRCUITS

Awake hippocampal reactivations project onto orthogonal neuronal assemblies

Arnaud Malvache,* Susanne Reichinnek,* Vincent Villette,* Caroline Haimerl, Rosa Cossart†

The chained activation of neuronal assemblies is thought to support major cognitive processes, including memory. In the hippocampus, this is observed during population bursts often associated with sharp-wave ripples, in the form of an ordered reactivation of neurons. However, the organization and lifetime of these assemblies remain unknown. We used calcium imaging to map patterns of synchronous neuronal activation in the CA1 region of awake mice during runs on a treadmill. The patterns were composed of the recurring activation of anatomically intermingled, but functionally orthogonal, assemblies. These assemblies reactivated discrete temporal segments of neuronal sequences observed during runs and could be stable across consecutive days. A binding of these assemblies into longer chains revealed temporally ordered replay. These modules may represent the default building blocks for encoding or retrieving experience.

The concept of "cell assembly" refers to a group of neurons that are coactivated repeatedly for a given brain operation (*1*). Cell assemblies thus represent a distinct cognitive entity embedded within neuronal networks (*2*). However, both their basic structural and functional organization, when outside world influences are minimal, as well as their long-term dynamics, remain unknown owing to the experimental difficulty of circumscribing them. In principle, the chained coordinated activation of such neuronal assemblies combines into sequences of neuronal activation supporting complex cognitive processes (*3*). Therefore, sequences of neuronal activation can represent a remarkable motif for revealing the activation of underlying neuronal assemblies. In the hippocampus, sequences occur at multiple time scales in the CA1 region—e.g., at the time frame of behavior—or compressed within the period of fast network oscillations (*2*, *4*). They can integrate time and/or distance, as well as any contextual information. Of particular interest are the coordinated patterns of neuronal activation that occur during awake immobility and that are related to sharp wave–associated ripples (SWRs), because these are produced when bodily or environmental control over hippocampal dynamics is minimal. Even though these coherent population events include sequential place cell reactivation representing past or future spatial experience, they are indeed also critically shaped by the internal functional organization of local circuits (*5*–*7*). Sequential neuronal reactivation can be split into separate chunks of current or remote experience (*8*–*11*), but their spatiotemporal organization into different cell assemblies remains unknown. So far, the dissection of hippocampal sequences into discrete reactivation patterns has been achieved by mapping them onto an external spatiotemporal template, such as an experienced behavior (*8*–*12*). It is important to minimize external sensory inputs to reveal the default organization of hippocampal dynamics into cell assemblies because local inputs are known to bias the content of both local and remote replay (*10*). We recently described a paradigm for revealing internally driven spatiotemporal sequences that occur during run behavior, which is particularly well suited to address this issue (*13*). However, monitoring large-scale multineuronal activity at high cellular density to identify cell assemblies represents a major technical challenge. This is particularly critical in the case of hippocampal population bursts, as they involve local microcircuits within the densely packed pyramidal layer (*7*, *14*). In vivo imaging of hippocampal dynamics is ideally suited to circumvent this limitation.

We used chronic two-photon calcium imaging of awake head-restrained mice allowed to self-regulate their motion in the dark on a nonmotorized treadmill (*13*). To map neuronal activity across consecutive days, we used a viral vector (AAV2/1.syn-GCaMP5G, -6m, and -6f; see table S1) (*15*) that allows for the detection of sparse firing through a glass window on the hippocampus (*16*), as described in (*17*). Additionally, mice were chronically implanted with an extracellular field electrode placed in the CA1 stratum pyramidale on the contralateral side to monitor the occurrence of network oscillations in the contralateral local field potential (LFP) during awake immobility periods. Particular attention was given to fast frequency domains (100 to 200 Hz) because most, but not all, CA1 population bursts that occur bilaterally during immobility are associated with SWRs. Because a fraction of awake SWRs is coherently observed in both hippocampi, supported by their anatomical interconnections (*18*), the contralateral LFP can be used as a reference to identify whether specific calcium transients are associated with the occurrence of SWRs. During each daily imaging session, mice spontaneously alternated between run and immobility epochs (Fig. 1A). Sequences of neuronal activation integrating spatiotemporal information (*13*) recurred during spontaneous run periods (RUN sequences) (Fig. 1A) (n = 3 out of 4 mice, table S1). During immobility periods, significant peaks of synchronous neuronal activity were observed (Fig. 1A)

INMED, INSERM U901, Aix-Marseille Université, Marseille, France.
*These authors contributed equally to this work. †Corresponding author: Email: rosa.cossart@inserm.fr